Modulation of recombination zone position for white perovskite/organic emitter hybrid light-emitting devices

Cite as: Appl. Phys. Lett. **120**, 093301 (2022); doi: 10.1063/5.0077633
Submitted: 4 November 2021 · Accepted: 13 February 2022 ·
Published Online: 28 February 2022

Xiang Zhang,[1,2,3] Xiaoheng Yan,[2] Lindsey J. Gray,[2] Junwei Xu,[4] Wenfa Xie,[3,a)] and David L. Carroll[2,a)]

AFFILIATIONS

[1]School of Microelectronics, Hefei University of Technology, Hefei 230009, China
[2]Center for Nanotechnology and Molecular Materials, Department of Physics, Wake Forest University, Winston-Salem, North Carolina 27105, USA
[3]State Key Laboratory of Integrated Optoelectronics, College of Electronics Science and Engineering, Jilin University, Changchun 130012, People's Republic of China
[4]Stanford Synchrotron Radiation Lightsource, SLAC National Accelerator Laboratory, Menlo Park, California 94025, USA

[a)]**Authors to whom correspondence should be addressed:** xiewf@jlu.edu.cn and carroldl@wfu.edu

ABSTRACT

Metal halide perovskites present specific challenges as emitters in large area, surface emission lighting devices. Among these challenges is the vast difference in carrier mobilities between the perovskite and many organic buffer layers typically used in such device fabrication as transport and blocking layers. This can make it difficult to engineer recombination to achieve white emitting devices generally. However, in this work, we introduce unique modulation of excitonic confinement within the perovskite layer of the device stack to control overall placement of the recombination zone. This results in a white light emitter that is bright and highly tunable, providing a path to realize white perovskite related light-emitting devices.

Metal halide perovskites have recently attracted considerable attention in optoelectronic applications, particularly in light-emitting devices (LEDs).[1–7] Due to advantages in cost, tunable bandgap, high recombination rate, high color purity, and high charge carrier mobilities, metal halide perovskite LEDs (PeLEDs) have quickly received research interest with some of the best reported external quantum efficiency (EQE) now over 20%.[8–10] However, compared with monochrome perovskite LEDs, white LEDs show special importance. This includes applications such as general illumination and backlighting in displays. Achieving white emission in a perovskite-based LED is, thus, an obvious and necessary next step in the development of this technology.

To date, some traditional methods for white lighting devices based on perovskite photoluminescence (PL) have been demonstrated.[11–16] The white LED realized by coupling a blue perovskite LED with a layer of a red perovskite down-converter has also been reported.[17] To realize the electroluminescence (EL), Chen *et al.* demonstrated a white perovskite LED based on a $CsPbI_3$ emissive layer with both α and δ phases.[18] For the device physics field, different color perovskites, such as blue and red perovskites, can be combined as emission layers to achieve white emission PeLEDs.[19] However, the shared interface has the problem of ion exchange reactions, which lead to unexpected color emission rather than white emission, as shown in Fig. 1(a).[20–22] Then an organic layer used as the buffer layer is necessary to avoid the ion exchange reactions. Aside from that, blending the perovskites with organic emitters to produce white emission was also researched.[23,24] However, the energy transfer is increasingly more efficient with decreasing intermolecular distance, leading to the blue emission quenching and reducing the probability of white emission generation.[23,25,26] Notably, highly efficient and stable blue perovskites still remain great challenges.[27–29] This, too, is not an ideal solution for a white perovskite related LED now.

Organic emitters with broad emission are more suitable for a high color rendering index (CRI) device. However, phosphor and thermally activated delayed fluorescence (TADF) materials with an internal quantum efficiency (IQE) of 100% always have slow recombination rate ($\sim\mu$s), leading to serious efficiency roll-off. While perovskite materials cannot only achieve an IQE of 100% but also have a

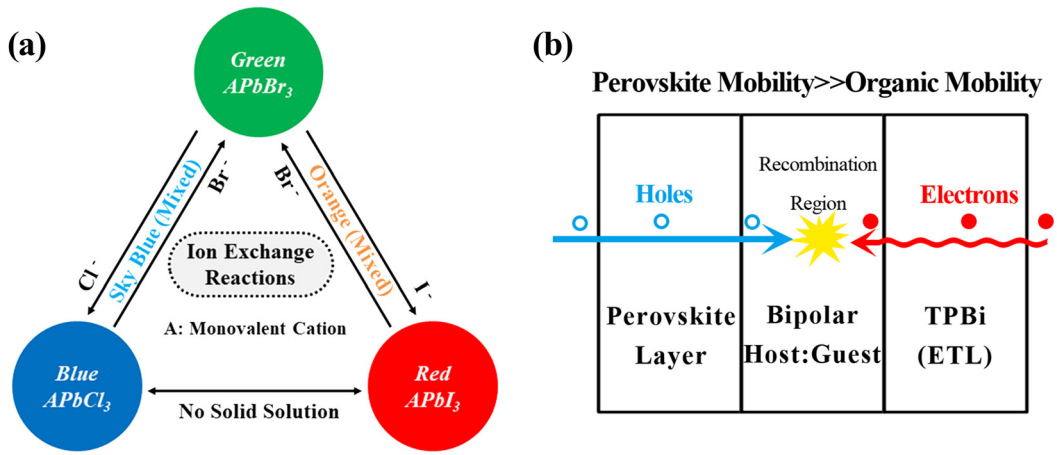

FIG. 1. (a) The schematic of the ion exchange reactions. (b) The working mechanism of the device when the mobility of perovskites is much higher than that of the organic emission layer.

fast recombination rate (~ns), it is considered that the combination of perovskite materials and organic emitters can address the trade-off issue between the high CRI and low efficiency-off. Then, increasing spatial separation using organic emitters stacked with bulk perovskites might be a workable approach to realize white perovskite/organic hybrid LEDs (Hyb-LEDs). Aside from avoiding some of the obvious limitations of the approaches above, there are several important aspects of this hybrid organic emitter-perovskite system that must be considered. Perhaps the most important is that the mobility of the perovskite is normally three or four orders of magnitude higher than those of organic materials.[30,31] An ideal bipolar host is difficult to synthesize and to obtain simultaneous luminescence from perovskites and organic emitters. Thus, the recombination may not occur at the area of the perovskite/organic interface due to the huge mobility difference between perovskites and organic materials, as shown in Fig. 1(b). Therefore, it can be difficult to make the perovskite/organic emission layers emit simultaneously in an electroluminescent device.

In this work, we propose a solution to this problem. We demonstrate a modulation of the recombination zone in stacked perovskite/organic co-emitting layers that is able to simultaneously realize luminescence. Based on P type and N type double hosts in the organic emission layer, the recombination zone position can be tuned by tuning the weight ratio between P and N type hosts and the thickness of the organic emission layer. Then the perovskite/organic emission layers emit simultaneously in the electroluminescent device. A highly efficient white Hyb-LED with 910 cd/m^2 luminance can be obtained with this approach. We believe our work would contribute to the understanding and controlling of the recombination region and provide a path for efficient white perovskite related LEDs.

The fabrication process and characterization of the device can be found in the supplementary material. As it is difficult to get co-emission from the perovskite/organic layers in an electroluminescent device, a possible approach is shown in Fig. 2(a), where recombination is forced to occur in a modulated recombination zone, similar in concept to a hybrid quantum well stack. A double-host in the organic emission layer, which contains both a P-type organic material, 4,4′,4″-Tris(carbazol-9-yl)triphenylamine (TcTa), and a N-type material, 1,3,5-Tris(1-phenyl-1Hbenzimidazol-2-yl)benzene (TPBi), modulates the recombination zone in the stacked emitting layers, facilitating stable co-emission from both the perovskite and the organic layer. Figure 2(a) shows the schematic illustration of perovskite/organic hybrid LEDs with a structure of ITO/Poly(3,4-ethylenedioxythiophene)-poly(styrenesulfonate) (PEDOT:PSS)/Cs-Pb-Br perovskite/organic emission layer/TPBi (30 nm)/LiF (1 nm)/Al (100 nm). Here, PEDOT:PSS (~40 nm) is used as a hole injection layer, and TPBi (30 nm) is used as an electron transport layer (ETL). Our independent variables are the weight ratio between the two hosts and the total solution concentrations of the organic emission layer. Table I shows the details of variables in the organic emission layer.

By dissolving $PbBr_2$ and CsBr in dimethyl sulfoxide (DMSO) at the molar ratio of 1:1.5, the Cs-Pb-Br perovskite films were fabricated by a spin-coating method. The absorbance and PL spectra of prepared Cs-Pb-Br perovskite films and organic emitters, Bis(3,5-difluoro-2-(2-pyridyl)phenyl-(2-carboxypyridyl)iridium(III) (FirPic) and Bis(2-methyldibenzo[f,h]quinoxaline)(acetylacetonate)iridium(III) [Ir(MDQ)$_2$(acac) or MDQ], are shown in Fig. 2(b). FirPic emits blue color, the Cs-Pb-Br perovskite film emits green color at 518 nm with a full width at half maximum (FWHM) of 20 nm, and Ir(MDQ)$_2$(acac) emits red color. The thickness of the perovskite was measured to be ~100 nm, and the photon recycling effect could contribute to the light extraction from LEDs.[32] In addition, the optical losses caused by the absorption of the perovskite layer are limited. The absorption of perovskites below 550 nm would be beneficial to the energy transfer from the blue Firpic to the green perovskite. The overlap between the perovskite PL spectrum and the Ir(MDQ)$_2$(acac) absorbance spectrum is really small, indicating that the energy transfer between them is very weak. The properties of the perovskite, like transmission electron microscopy or atomic force microscopy images, have already been discussed in our previous work.[33] The morphology of the Cs-Pb-Br perovskite film deposited on PEDOT:PSS, which measured by a top-view scanning electron microscope (SEM), has been shown in Fig. S1. We also used grazing incidence wide-angle x-ray scattering (GIWAXS) measurement, and the result is shown in Fig. 2(c). The result exhibits a ring-like Debye Scherer pattern, indicating a randomly oriented crystal. After spin-coating the organic

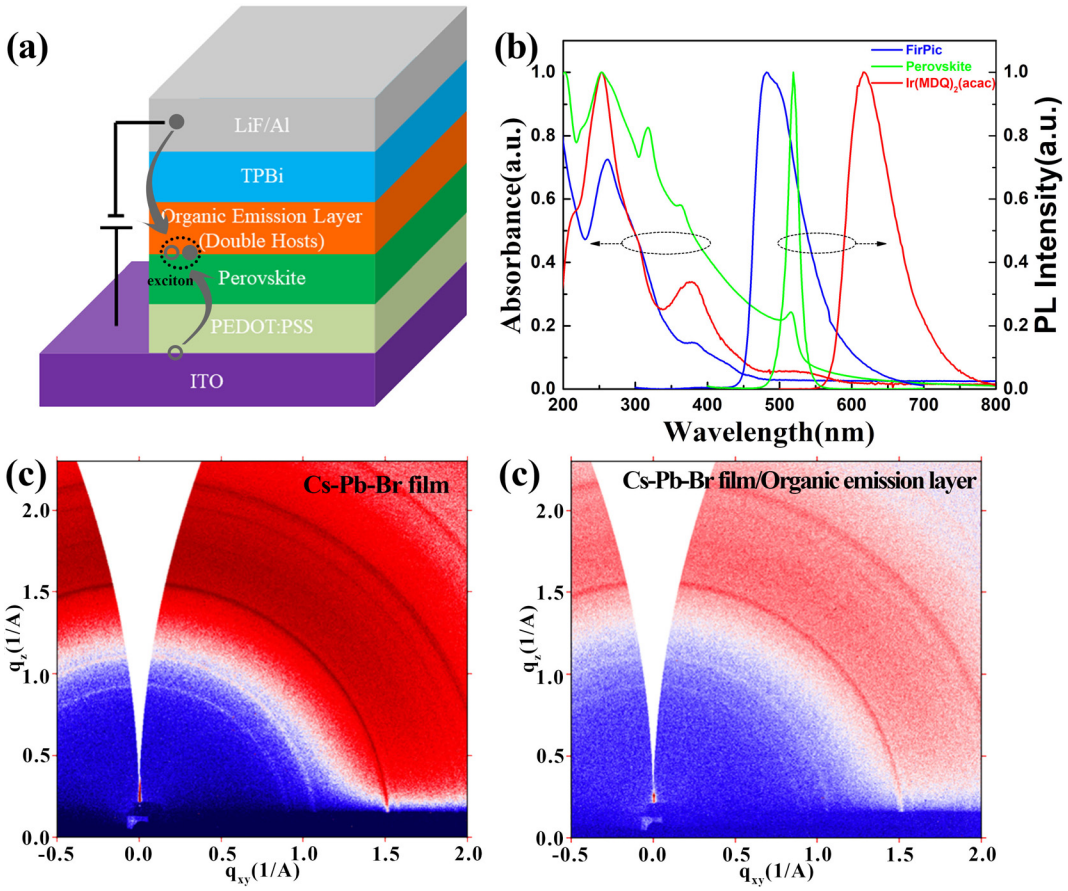

FIG. 2. (a) The device structure used in this paper. (b) The absorbance and PL spectra of perovskites, FirPic and $Ir(MDQ)_2(acac)$. The GIWAXS result of the (c) perovskite film and (d) perovskite/organic emission layer.

emission layer on top of the perovskite layer, a ring-like Debye Scherer pattern can also be observed in Fig. 2(d). Thus, solution-processible fabrication of the organic emission layer has trivial effects on the crystallinity of the Cs-Pb-Br perovskite film.

As shown in Table I, when the weight ratio of TcTa and TPBi changed from 1:0–1:4 to 0:1, these devices were labeled in sequence from device A to device F. The thickness of these organic emission layers here were measured to be ~40 nm, and the performance of these devices is shown in Fig. S2. Figures 3(a)–3(f) show the EL spectra variation under the same voltage of these devices. Here, device A means only TcTa used as the host in the organic emission layer, and the spectrum in Fig. 3(a) indicates only red color emitted from $Ir(MDQ)_2(acac)$ can be seen. With the increase in the TPBi content, green emission from the perovskite layer becomes dominant in the

TABLE I. The composition of the organic emission layer in different devices.

Name	Organic emission layer	Weight ratio	Concentration
Device A	TcTa:TPBi:5wt%MDQ	1:0	10 mg/ml
Device B	TcTa:TPBi:5wt%MDQ	1:1	10 mg/ml
Device C	TcTa:TPBi:5wt%MDQ	1:4	10 mg/ml
Device D	TcTa:TPBi:5wt%MDQ	1:9	10 mg/ml
Device E	TcTa:TPBi:5wt%MDQ	1:14	10 mg/ml
Device F	TcTa:TPBi:5wt%MDQ	0:1	10 mg/ml
Device G	TcTa:TPBi:5wt%MDQ	1:1	5 mg/ml
Device H	TcTa:TPBi:20wt%FirPic:0.5 wt%MDQ	1:2	10 mg/ml

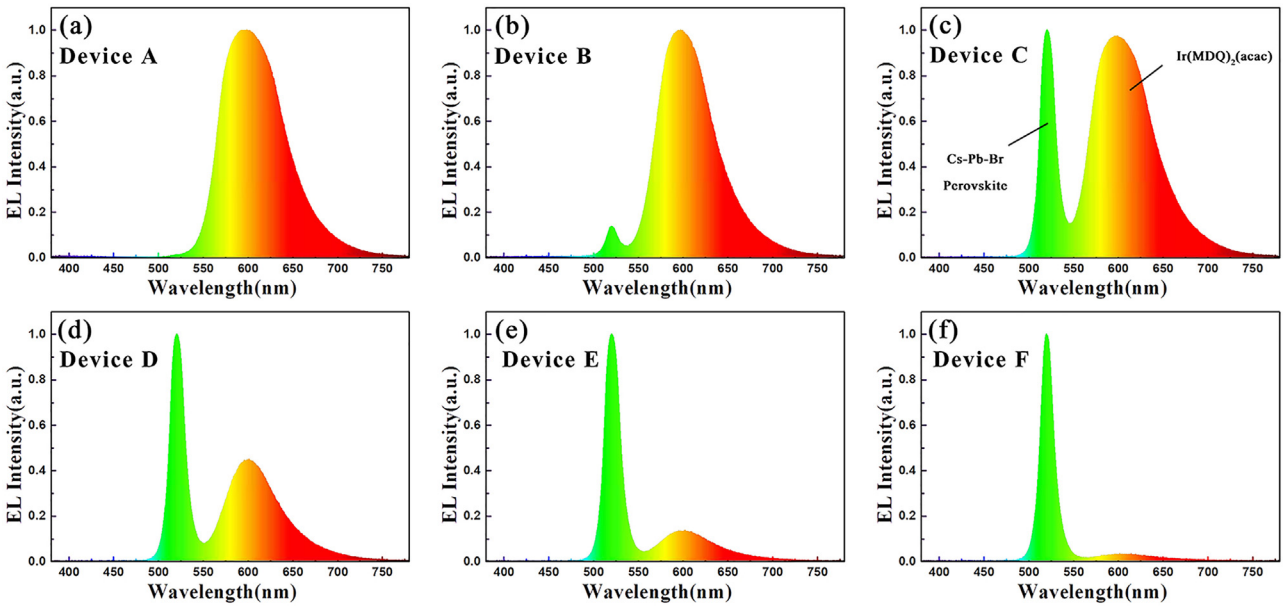

FIG. 3. The EL spectra of (a) device A, (b) device B, (c) device C, (d) device D, (e) device E, and (f) device F under the same voltage.

emission spectrum. As shown in Fig. 3(c), the intensity of green and red color was comparable for device C. If the TPBi content further increased to only TPBi used as the host, which means the weight ratio of TcTa and TPBi was 0:1, the green color intensity of device F was significantly higher than that of red color, and the red color intensity was extremely weak as shown in Fig. 3(f). The change of emission color is denoted in the Commission Internationale de L'Eclairage (CIE) coordinates, which is shown in Fig. S3. The color of these devices changed from red through yellow to green, which indicates that the recombination zone position can be modulated by the weight ratio between P and N type hosts.

To study the physical mechanism, the distributions of electrons and holes of the devices with different weight ratios of TcTa and TPBi in the organic emission layer have been simulated by the drift-diffusion EL model, as shown in Fig. S4. Figure 4(a) shows the ratio of the electron density/hole density. It can be seen that the region of the balanced electron density and the hole density mainly concentrated at the interface of the organic emission layer and ETL for devices with P type host. The region of the balanced electron density and hole density shifts toward the anode side for devices with double hosts. For the device with N type host, the interface of the perovskite/organic emission layer is the region of the balanced electron density and hole density. Figs. 4(b)–4(d) display the schematic illustration for the modulation of the recombination zone position. For device A, as shown in Fig. 4(b), P type host TcTa can be used for hole transport and electron confinement. The injected holes from the anode would be transported through the Cs-Pb-Br perovskite and the organic emission layer and then confined by the TPBi ETL. The injected electrons from the cathode would be transported through the TPBi ETL and confined by the TcTa host. Thus, the recombination region was in the organic emission layer, leading to only red emission from $Ir(MDQ)_2(acac)$, as shown in Fig. 3(a). When N type TPBi was introduced into the organic emission layer, electrons can be transported in the organic emission layer due to the carrier transport characteristic of TPBi. Figure 4(c) indicates that the recombination zone position would move toward the anode direction with the increase in the TPBi content. For device C, the recombination region was in the organic emission layer and near the interface of the Cs-Pb-Br perovskite, corresponding to the spectrum in Fig. 3(c). Figure 4(d) shows that the recombination region was in the perovskite layer and the perovskite/organic interface for device F. Most of the injected holes were recombined with the injected electrons in the perovskite layer. However, a few holes manage to recombine with electrons at the perovskite/organic interface, resulting in dim emission of red color in Fig. 3(f). This is because the carrier mobility of inorganic perovskites is much higher than those of organic materials.

We further note that the thickness of the organic emission layer can also be adjusted to modulate the recombination region. Here, the thickness of the organic emission layer was adjusted by the concentration of the solution. The device with the organic emission layer made from a 5 mg/ml concentration solution was labeled as device G. The thickness was measured to be ~25 nm. For device B, as shown in Fig. 5(a), the intensity of red color is obviously higher than that of green color. The reason for this phenomenon is that most of the recombination zone position was located in the organic emission layer due to the thick organic emission layer, as shown in Figs. 5(c) and 5(d). When we decrease the thickness of the organic emission layer by decreasing the concentration of the solution, the recombination region would shift toward the perovskite layer. As shown in Fig. 5(b), the intensity of green color was comparable with the intensity of red color for device G. This is because more electrons can be transported into the perovskite layer, and the recombination region was modulated to the area near the perovskite/organic interface, as shown in Figs. S5, 5(c), and 5(d).

Based on above discussions, the recombination zone position can be finetuned according to the demand. To realize white perovskite/organic emitter hybrid LEDs, FirPic was introduced into the organic

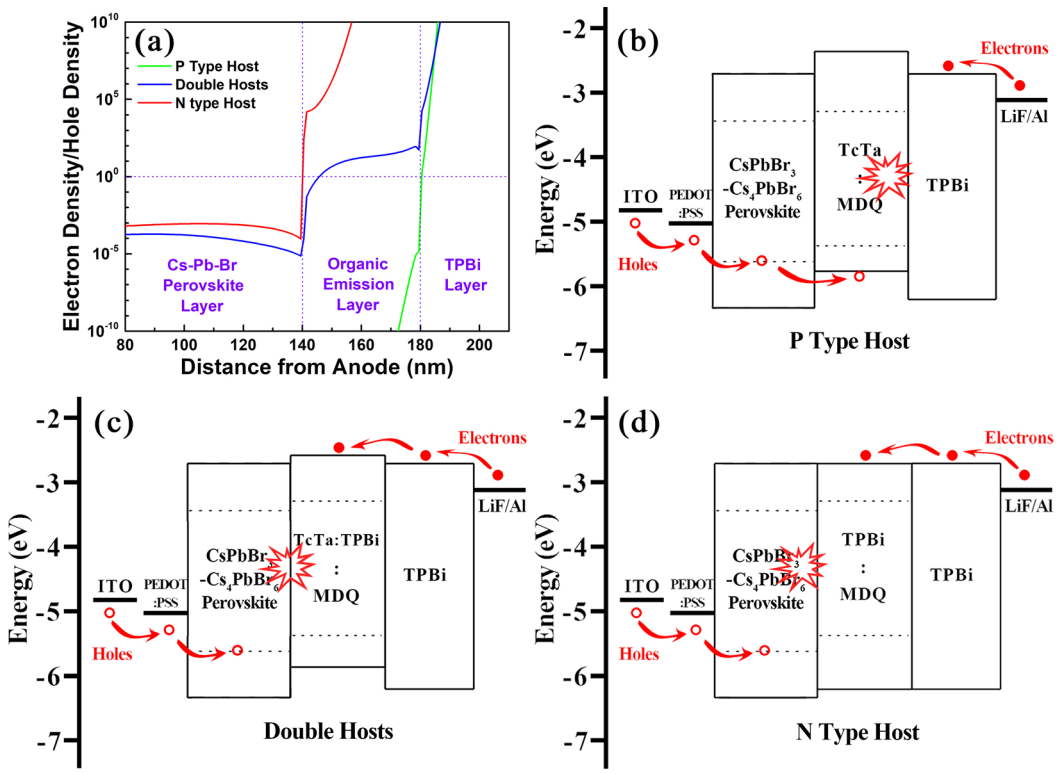

FIG. 4. (a) The electron density/hole density curves of device A, device C, and device F under the same voltage. The working mechanism of (b) device A, (c) device C, and (d) device F.

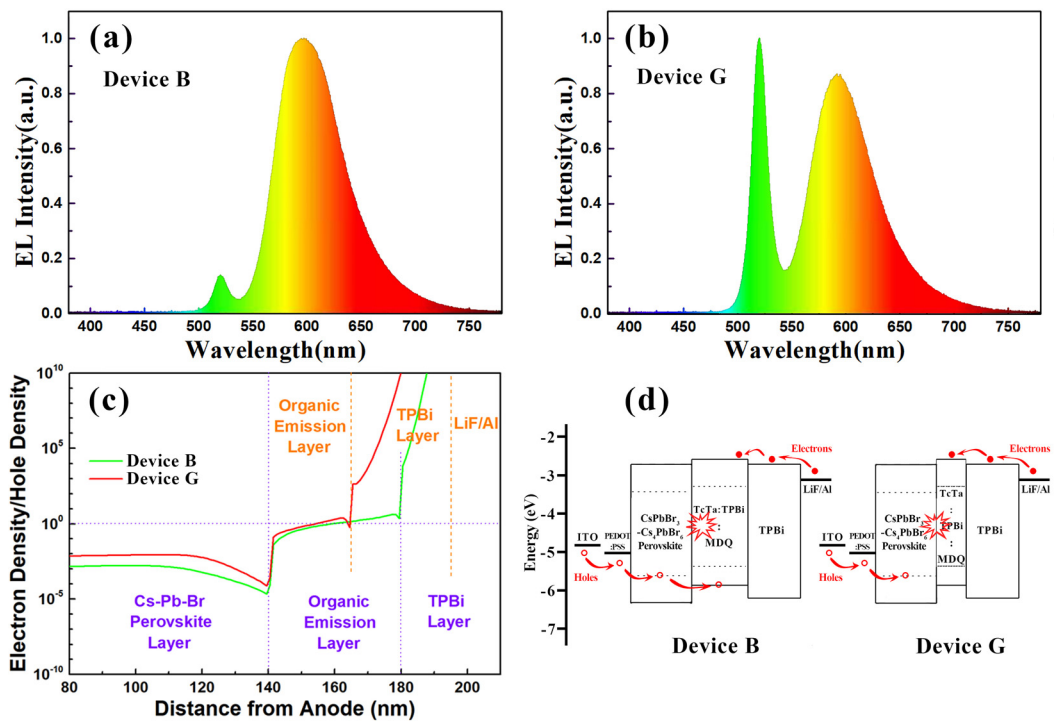

FIG. 5. The EL spectra of (a) device B and (b) device G. (c) The electron density/hole density curves and (d) the work mechanism of device B and device G under the same voltage.

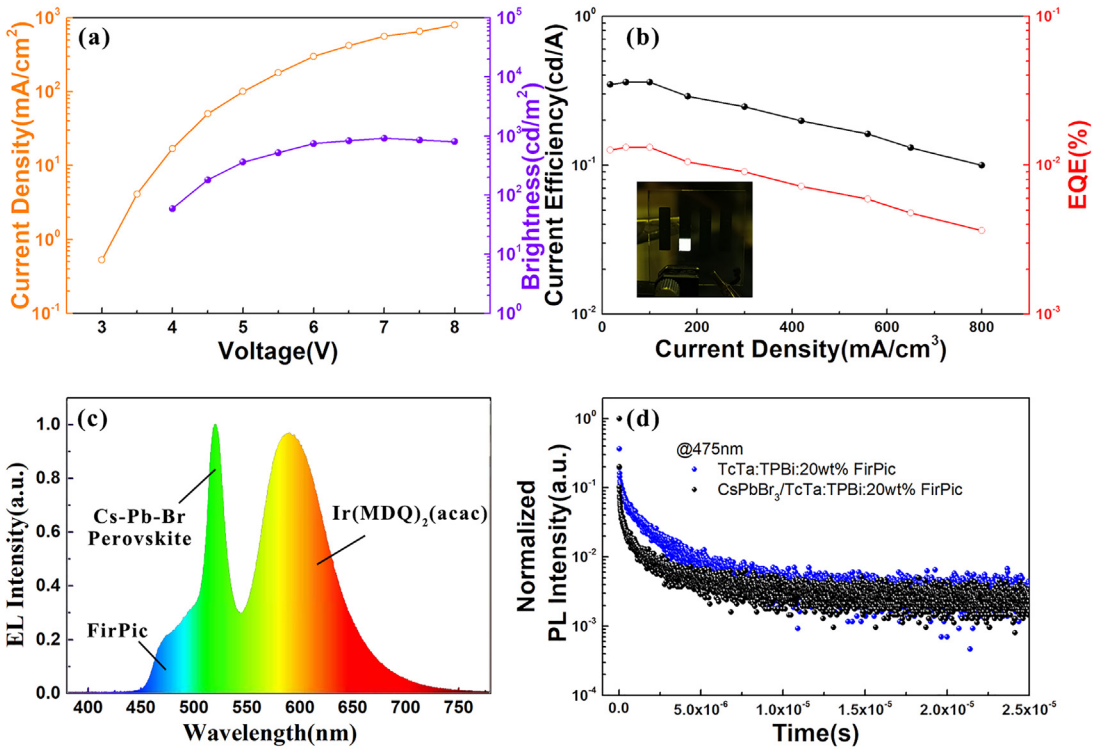

FIG. 6. (a) Current density–voltage–brightness curve and (b) current efficiency–current density–EQE curve of device H. Insert: The photo of device H. (c) The EL spectrum of device H and (d) transient PL decay curves of different emitting layers.

emission layer, and the device was labeled as device H. The organic emission layer of device H was TcTa:TPBi:20wt%FirPic:0.5 wt. % $Ir(MDQ)_2(acac)$, and the weight ratio of TcTa and TPBi was 1:2, as shown in Table I. Figures 6(a) and 6(b) show the performance of device H. The maximum brightness of device H was 910 cd/m^2. The maximum current efficiency and EQE of device H were 0.36 cd/A and 0.013%, respectively. The spectrum of device H is shown in Fig. 6(c), and around 3000 K color temperature white Hyb-LEDs with CRI of 71 were achieved as shown in Fig. S6. The CRI of the device could be further improved to over 80 by using other materials, like deep-blue emitters or TADF emitters with a wide spectrum. Figure 6(d) displays the transient PL decay of different emitting layers to understand the role of subsequent layers and organic/perovskite layer interfaces. The introduction of additional Cs-Pb-Br perovskite layer accelerates the decay of blue emission from the FirPic molecules. Thus, energy transfer could be observed from the FirPic to perovskite. The energy transfer between FirPic and $Ir(MDQ)_2(acac)$ has been widely discussed in the reported literature.[34] Due to these energy transfer, the intensity of blue color emission was lower than that of green and red color, which is beneficial to reduce the blue light hazard.[35,36] It has also been confirmed by comparison of the EL spectra. Figure S7 shows the EL spectrum of the device without the perovskite layer, and the intensity of FirPic is comparable with the intensity of $Ir(MDQ)_2(acac)$. Due to the thin film (~100 nm), the optical losses caused by the absorption of the perovskite layer are limited. Then, energy transfer plays a more important role. Therefore, highly efficient white perovskite/organic emitter hybrid LEDs with low color temperatures were realized through modulation of the recombination zone position. We believe our work would contribute to the understanding and controlling of the recombination region and provide a path for efficient white Hyb-LEDs with the "green perovskite/blue organic emitter/red perovskite" structure, which can avoid both ion exchange reactions and the difficulty of blue perovskites.

In summary, modulation of the recombination zone position for perovskite/organic emitter hybrid light-emitting devices had been proposed. Based on P type and N type double hosts in the organic emission layer, the recombination region can be adjusted by tuning the weight ratio between P and N type hosts and changing the thickness of the organic emission layer. Then, the highly efficient white perovskite/organic emitter hybrid light-emitting device was realized with this method. The maximum brightness reached 910 cd/m^2, and the maximum current efficiency reached 0.36 cd/A. We believe our work would contribute to the understanding and controlling of the recombination region and provide a path for white Hyb-LEDs with the structure of "green perovskite/blue organic emitter/red perovskite," which can avoid both ion exchange reactions and the difficulty of blue perovskites.

See the supplementary material for the experimental method and more characterizations.

The authors acknowledge the support from NSF through Grant No. ECCS-1610641. X.Z. acknowledges the support from the program of China Scholarship Council (No. 201906170195). The authors thank Dr. Shihao Liu for helpful discussions.

AUTHOR DECLARATIONS

Conflict of Interest

The authors have no conflicts to disclose.

DATA AVAILABILITY

The data that support the findings of this study are available from the corresponding author upon reasonable request.

REFERENCES

[1]C. Zhang, D. B. Kuang, and W. Q. Wu, Small Methods **4**(2), 1900662 (2020).
[2]Y. Li, X. Zhang, H. Huang, S. V. Kershaw, and A. L. Rogach, Mater. Today **32**, 204 (2020).
[3]Q. Shan, J. Song, Y. Zou, J. Li, L. Xu, J. Xue, Y. Dong, B. Han, J. Chen, and H. Zeng, Small **13**(45), 1701770 (2017).
[4]Q. Van Le, H. W. Jang, and S. Y. Kim, Small Methods **2**(10), 1700419 (2018).
[5]M. Lu, Y. Zhang, S. Wang, J. Guo, W. W. Yu, and A. L. Rogach, Adv. Funct. Mater. **29**(30), 1902008 (2019).
[6]H. Cho, Y. H. Kim, C. Wolf, H. D. Lee, and T. W. Lee, Adv. Mater. **30**(42), 1704587 (2018).
[7]L. N. Quan, F. P. García de Arquer, R. P. Sabatini, and E. H. Sargent, Adv. Mater. **30**(45), 1801996 (2018).
[8]K. Lin, J. Xing, L. N. Quan, F. P. G. de Arquer, X. Gong, J. Lu, L. Xie, W. Zhao, D. Zhang, and C. Yan, Nature **562**(7726), 245 (2018).
[9]Y. Cao, N. Wang, H. Tian, J. Guo, Y. Wei, H. Chen, Y. Miao, W. Zou, K. Pan, and Y. He, Nature **562**(7726), 249 (2018).
[10]W. Xu, Q. Hu, S. Bai, C. Bao, Y. Miao, Z. Yuan, T. Borzda, A. J. Barker, E. Tyukalova, and Z. Hu, Nat. Photonics **13**(6), 418 (2019).
[11]M. Bidikoudi, E. Fresta, and R. Costa, Chem. Commun. **54**(59), 8150 (2018).
[12]C. Sun, Y. Zhang, C. Ruan, C. Yin, X. Wang, Y. Wang, and W. W. Yu, Adv. Mater. **28**(45), 10088 (2016).
[13]J. Luo, X. Wang, S. Li, J. Liu, Y. Guo, G. Niu, L. Yao, Y. Fu, L. Gao, and Q. Dong, Nature **563**(7732), 541 (2018).
[14]H. Wu, S. Wang, F. Cao, J. Zhou, Q. Wu, H. Wang, X. Li, L. Yin, and X. Yang, Chem. Mater. **31**(6), 1936 (2019).
[15]E. R. Dohner, A. Jaffe, L. R. Bradshaw, and H. I. Karunadasa, J. Am. Chem. Soc. **136**(38), 13154 (2014).
[16]T. Guner and M. M. Demir, Phys. Status Solidi A **215**(13), 1800120 (2018).
[17]Z. Chen, Z. Li, Z. Chen, R. Xia, G. Zou, L. Chu, S.-J. Su, J. Peng, H.-L. Yip, and Y. Cao, Joule **5**(2), 456 (2021).
[18]J. Chen, J. Wang, X. Xu, J. Li, J. Song, S. Lan, S. Liu, B. Cai, B. Han, and J. T. Precht, Nat. Photonics **15**(3), 238 (2021).
[19]J. Mao, H. Lin, F. Ye, M. Qin, J. M. Burkhartsmeyer, H. Zhang, X. Lu, K. S. Wong, and W. C. Choy, ACS Nano **12**(10), 10486 (2018).
[20]G. Nedelcu, L. Protesescu, S. Yakunin, M. I. Bodnarchuk, M. J. Grotevent, and M. V. Kovalenko, Nano Lett. **15**(8), 5635 (2015).
[21]G. Li, J. Y.-L. Ho, M. Wong, and H. S. Kwok, J. Phys. Chem. C **119**(48), 26883 (2015).
[22]D. M. Jang, K. Park, D. H. Kim, J. Park, F. Shojaei, H. S. Kang, J.-P. Ahn, J. W. Lee, and J. K. Song, Nano Lett. **15**(8), 5191 (2015).
[23]E. P. Yao, Z. Yang, L. Meng, P. Sun, S. Dong, Y. Yang, and Y. Yang, Adv. Mater. **29**(23), 1606859 (2017).
[24]C.-Y. Chang, A. N. Solodukhin, S.-Y. Liao, K. Mahesh, C.-L. Hsu, S. A. Ponomarenko, Y. N. Luponosov, and Y.-C. Chao, J. Mater. Chem. C **7**(28), 8634 (2019).
[25]I.-W. Cho and M.-Y. Ryu, Sci. Rep. **9**(1), 18433 (2019).
[26]A. Singldinger, M. Gramlich, C. Gruber, C. Lampe, and A. S. Urban, ACS Energy Lett. **5**(5), 1380 (2020).
[27]N. K. Kumawat, X.-K. Liu, D. Kabra, and F. Gao, Nanoscale **11**(5), 2109 (2019).
[28]T. Fang, F. Zhang, S. Yuan, H. Zeng, and J. Song, InfoMat. **1**(2), 211 (2019).
[29]Z. Li, Z. Chen, Y. Yang, Q. Xue, H.-L. Yip, and Y. Cao, Nat. Commun. **10**(1), 1027 (2019).
[30]J. Zeng, X. Li, Y. Wu, D. Yang, Z. Sun, Z. Song, H. Wang, and H. Zeng, Adv. Funct. Mater. **28**(43), 1804394 (2018).
[31]Z. Yu, H. Feng, J. Zhang, S. Liu, Y. Zhao, L. Zhang, and W. Xie, J. Mater. Chem. C **7**(30), 9301 (2019).
[32]C. Cho, B. Zhao, G. D. Tainter, J.-Y. Lee, R. H. Friend, D. Di, F. Deschler, and N. C. Greenham, Nat. Commun. **11**, 611 (2020).
[33]J. Xu, W. Huang, P. Li, D. R. Onken, C. Dun, Y. Guo, K. B. Ucer, C. Lu, H. Wang, S. M. Geyer, R. T. Williams, and D. L. Carroll, Adv. Mater. **29**(43), 1703703 (2017).
[34]S. Liu, X. Zhang, M. Yin, H. Feng, J. Zhang, L. Zhang, and W. Xie, ACS Appl. Energy Mater. **1**(1), 103 (2018).
[35]C. Gao, Z. Xiong, Z. He, Y. Dong, F. Yu, X. Ma, Y. Zhang, D. Zhou, and Z. Xiong, J. Mater. Chem. C **7**(28), 8705 (2019).
[36]J. H. Jou, C. Y. Hsieh, J. R. Tseng, S. H. Peng, Y. C. Jou, J. H. Hong, S. M. Shen, M. C. Tang, P. C. Chen, and C. H. Lin, Adv. Funct. Mater. **23**(21), 2750 (2013).